ISTITUTO NAZIONALE DI FISICA NUCLEARE - ISTITUTO NAZIONALE DI FISICA NUCLEARE - ISTITUTO NAZIONALE DI FISICA NUCLEARE - ISTITUTO NAZIONALE DI FISICA NUCLEARE - ISTITUTO NAZIONALE DI FISICA NUCLEARE - ISTITUTO NAZIONALE DI

Laboratori Nazionali di Frascati

Submitted to Nucl. Phys. & Meth. in Physics Research

LNF-93/016 (P)
29 Aprile 1993

A. Ferrari, M. Pelliccioni, P.R. Sala:

ESTIMATION OF FLUENCE RATE AND ABSORBED DOSE RATE DUE TO GAS BREMSSTRAHLUNG FROM ELECTRON STORAGE RINGS

PACS.: 28.80

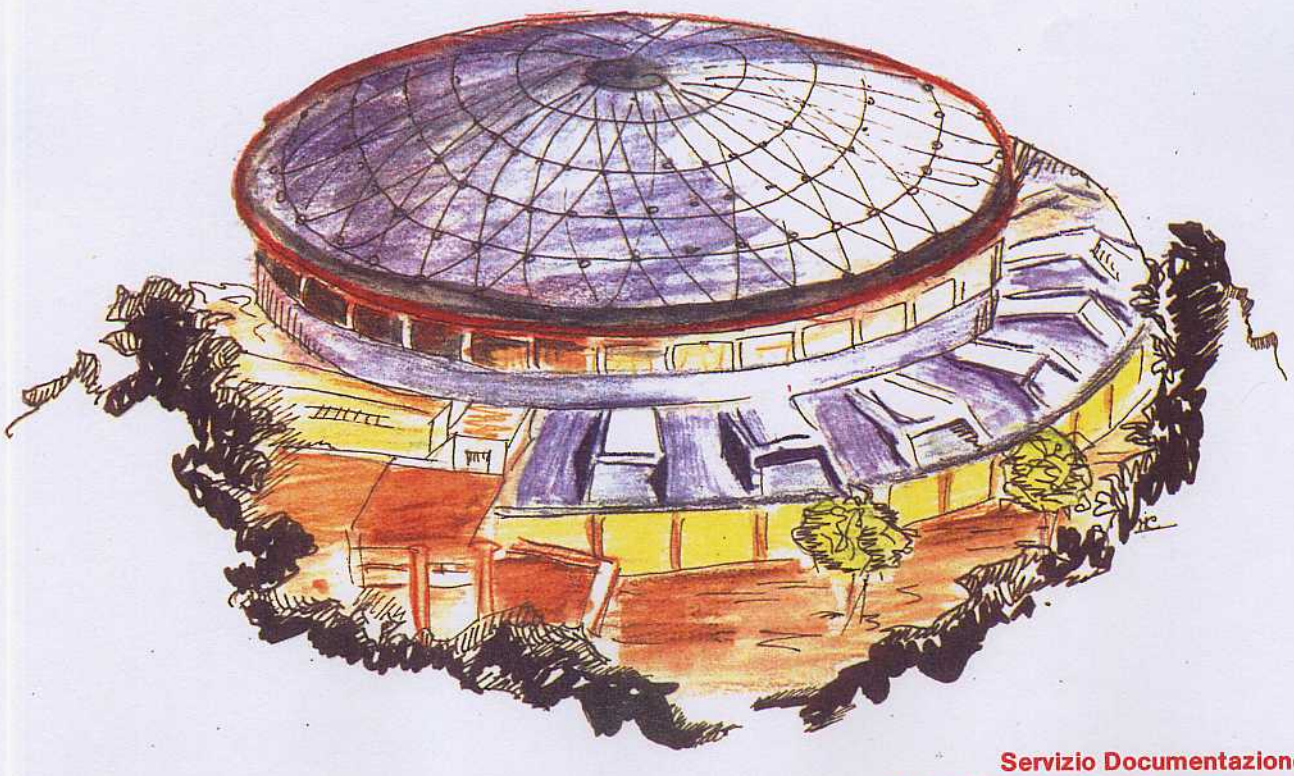

Servizio Documentazione
dei Laboratori Nazionali di Frascati
P.O. Box, 13 - 00044 Frascati (Italy)

INFN – Laboratori Nazionali di Frascati
Servizio Documentazione

LNF-93/016 (P)
29 Aprile 1993

ESTIMATION OF FLUENCE RATE AND ABSORBED DOSE RATE DUE TO GAS BREMSSTRAHLUNG FROM ELECTRON STORAGE RINGS

M. Pelliccioni
INFN, Laboratori Nazionali di Frascati, P.O. Box 13, I–00044 Frascati (Roma) Italia

A. Ferrari, P.R. Sala
INFN, Sezione di Milano, Via Celoria 16, I–20133 Milano Italy

ABSTRACT

Bremsstrahlung produced in electron storage rings by interactions with residual gas has been studied in the energy range 100–1000 MeV using the FLUKA code. Photon spectra and quantitative estimates of fluence rate and tissue absorbed dose rate are given. Simple equations are proposed for the fluence rate and the absorbed dose rate according to the results obtained.

INTRODUCTION

Bremsstrahlung on residual gas is one of the main sources of beam losses in electron–positron storage rings. Although the interactions of the primary particles with gas molecules or ions take place all around the machine, the photon intensity is especially high in straight sections. In fact in each interaction bremsstrahlung is produced in a narrow cone around the same direction and each contribution adds up to form a "hot spot" of dose somewhere at the end of the beam line. This narrow "jet" of bremsstrahlung X–rays may represent a serious radiation hazard when channeled outside the ring through the shield or when the shield itself is not thick enough.

Absorbed doses due to the gas bremsstrahlung have been measured with various methods at several facilities (1,2,3,4,5,6,7) and quantitative estimates have been carried out by various authors (6,8,9,10,11,12). Yet the results obtained are not exhaustive.

Recently quantitative estimates have been published using the Monte Carlo code EGS4 (13). However the results of these calculations and the proposed semiempirical expressions are not completely satisfactory.

Therefore we have studied again the radiation protection aspects of the gas bremsstrahlung emission in storage rings, with the aim to find some practical expressions linking absorbed dose rate or photon density fluence to the various parameters. We have limited our study to the intermediate energy region (100–1000 MeV), which is particularly interesting for a new stimulating utilization of the storage rings, the Φ–factories (510 MeV).

We have used the code FLUKA (14) in its most recent version, which includes major modifications to the original one (15,16,17). In particular, the treatment of bremsstrahlung is completely new, as photon yield and spectra are now based on the tabulations of Seltzer and Berger (18), and the photon angular distributions are accurately described.

DETAILS OF THE SIMULATION

In the simulations a storage ring straight section is represented by an air target hit by a pencil electron beam. Though the chemical composition of the residual gas in a storage ring might be different from that of the air, the equivalence in terms of average values of the atomic number has been verified (1).

Unlike other codes (included the standard version of EGS4) where the photons are considered emitted at a fixed angle, the characteristic angle $\theta_c=mc^2/E$, mc^2 being the electron rest mass and E the electron beam energy, FLUKA allows to take into account the true angular distribution of the emitted photons for arbitrary screening through the use of Thomas–Fermi–Molière atomic form factors inside the formula 2CS of ref. (22) (see ref. (17) for the details of the algorithm implemented in FLUKA). The need for such a key improvement has been recently realized by the EGS4 developers, who introduced a suitable algorithm into their code (23).

To overcome the difficulties due to the low interaction probability at the operating pressure of a storage ring $1.33\cdot10^{-7}$ –10^{-8} Pa (10^{-9}–10^{-10} torr), calculations have been performed with the gas density corresponding to the atmospheric pressure. The obtained results have been linearly scaled with the pressure.

This procedure takes properly into account the dependence of the photon yield on the residual gas pressure, but not the differences in the angular distributions due to electron scattering effects like, for instance, the multiple Coulomb scattering and the Möller scattering. The former broadens the angular distribution of the emitted photons but does not affect their number. Since the multiple scattering is practically negligible in the vacuum chamber of a storage ring, while it is responsible of the large broadening of the beam at atmospheric pressure, it has been suppressed in our simulation with FLUKA.

Moreover, the threshold for the Möller scattering of the electrons has been set at 10 MeV to minimize any angular deflection due to the production of δ–rays.

The proper simulation of the angular distribution of the emitted photons and the precautions to avoid spurious widening due to scattering processes are indeed of great

importance in getting meaningful results for this particular problem. The neglect of these two aspects leads to completely fictitious "angular distributions" which are actually the folding of a δ distribution (centered on the characteristic angle if using EGS4), with the multiple scattering distribution of the emitting electrons into an air target at atmospheric pressure (an example of these fictitious distributions is the one plotted in Fig. 3 of ref. (13)).

However, the procedure of scaling the results of the simulation with pressure cannot be applied to very long straight sections. Its limits of validity are set by two requirements: the former is that the probability of reinteraction of photons in the target must be negligible, the latter is that the longitudinal distribution of electron interaction in the target must be uniform, as it is at very low pressure. This second condition is fulfilled if the electron interaction probability is less than few percent, or, equivalently, if the average electron energy loss is a small fraction of the beam energy.

The failure of these conditions has been observed with targets longer than about 10 m. Therefore for these targets the simulation has been carried out at 1/10 of the atmospheric pressure.

We considered straight section lengths ranging from 1 to 50 metres. This range includes the typical straight sections of the storage rings dedicated to the synchrotron radiation and of Φ–factories.

The photon fluence has been scored at nine distances from 1 m to 500 m from the end of the target simulating the straight section. Afterwards, further runs have been carried out also at distances shorter than 1 m, with the aim to extend the validity of the equations proposed for linking photon density fluence and absorbed dose rate to the various parameters.

In order to evaluate doses at a given distance, photon fluences were converted into tissue absorbed doses using the conversion coefficients suggested by Rogers (19). The results should be conservative because these conversion coefficients are for a broad parallel beam, whereas the gas bremsstrahlung beam is confined to a very narrow cone.

The code energy cuts were 10 MeV for charged particles and 10 keV for photons. To avoid large statistical uncertainties in the Monte–Carlo results, the number of primary electrons followed was always at least 700000. In some cases we followed up to 1200000 electrons.

Some remarks are necessary about the size of the scoring area. This aspect has been already studied in a previous note dedicated to a similar problem, the choice of the source terms at 0° in the case of targets bombarded by high energy electrons (20). The computed photon fluence rate and absorbed dose rate saturate only at scoring angles significantly smaller than the characteristic one. This behaviour is in agreement with the theoretical expression for the photon angular distribution, whose leading term is of the form $1 / [\, 1 + (\theta / \theta_c)^2 \,]^2$.

Therefore the scoring area has to be as large as possible to save CPU time, but small enough to avoid underestimates of fluences and absorbed doses.

In order to take this into account, we have placed at each of the nine investigated locations 14 concentric scoring detectors of radius ranging from 0.0005 cm to 10 cm. The saturation values at each location have been easily determined by looking at the behaviour of the fluence (or the absorbed dose) versus the detector radius.

As an example, Fig. 1 shows the tissue absorbed dose rate per e^-/s for a 510 MeV beam as a function of the detector radius at various distances from the end of a 3.7 m long straight section operating at a pressure of $1.33 \cdot 10^{-7}$ Pa (10^{-9} torr). The statistical uncertainty in the results shown is comprised between 0.3% and 9%. As the distance from the straight section increases, the data of the smallest detectors are omitted, because their evaluation with sufficient accuracy would have required unmanageable CPU times.

It is evident from the curves in Fig. 1 that the choice of exceedingly large scoring angles, or the use of large detectors in experimental measurements, would lead to significant underestimates, and that it is definitely not sufficient to require that the scoring area must be in the radiation cone, defined by the characteristic angle, as suggested for instance in ref. (13).

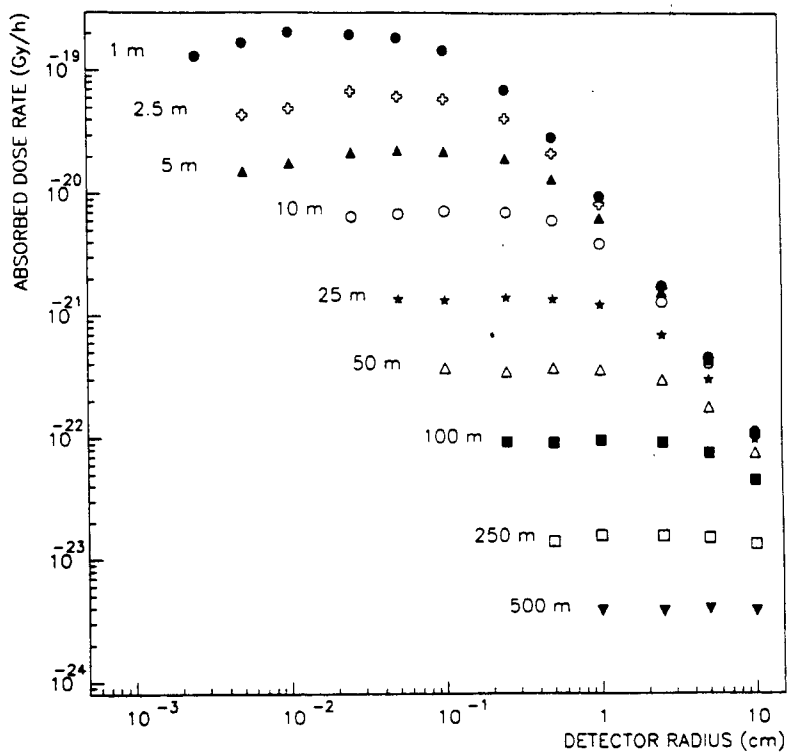

FIG. 1 – Absorbed dose rate per e^-/s as a function of the radius of the scoring area at various distances from a straight section 3.7 m long operating at a pressure of $1.33 \cdot 10^{-7}$ Pa (10^{-9} torr). Primary electron energy 510 MeV.

RESULTS AND DISCUSSION

First of all the behaviour of the fluence rate and absorbed dose rate as a function of the distance from the end of the air target and of its length has been studied. This study has been performed at 510 MeV, the energy of the storage rings at present under construction as Φ–factories. Afterwards, the dependence of these quantities on the electron energy has been investigated.

As an example, Fig. 2 shows the bremsstrahlung energy spectra, in terms of fluence rate per e^-/s, generated with different beam energies. These spectra have been scored at a

distance of one metre from the end of an one metre long straight section at a pressure of $1.33 \cdot 10^{-7}$ Pa (10^{-9} torr). They are obtained by scaling linearly the results of a simulation at atmospheric pressure, using the precautions described in the previous chapter. They can be considered representative of the real spectra at $1.33 \cdot 10^{-7}$ Pa (10^{-9} torr) because the target is short (1 m) and the selected scoring areas small enough (0.0059 cm^2 at energies greater than 500 MeV; 0.16 cm^2 at 250 MeV; 0.59 cm^2 at 100 MeV). Some spectra seem to extend up to energies higher than the energy of the primary electron beam, but this is only an effect of the adopted energy binning, whose edges do not always match the primary electron energy.

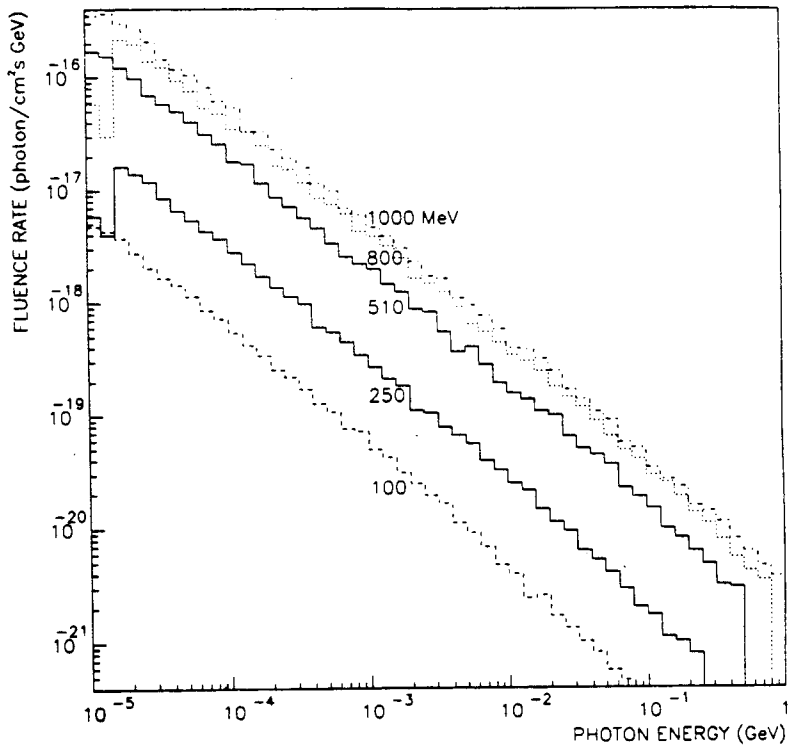

FIG. 2 – Photon spectra in terms of fluence rate per e^-/s as recorded at a distance of 1 m from a straight section 1 m long operating at a pressure of $1.33 \cdot 10^{-7}$ Pa (10^{-9} torr) for various primary electron energies.

The dependence of fluence rate and absorbed dose rate on the various parameters are very similar. The dependence of both quantities on the length of the air target is weak for small distances (≤10 m), while it becomes important at larger distances (≥10 m).

We have checked whether the bremsstrahlung emission can be approximated by a point source placed at the centre of the straight section and whether the inverse square law is valid, as suggested by other authors (13). We have found that these properties are valid for a 1 metre long straight section, the same length investigated by the authors above mentioned. For longer straight sections, the point source moves towards the end of the straight section. It should be located at about 2/3 and 3/4 of the target length for straight sections of 3.7 m and about 15 m, respectively.

Actually, the dependence on the geometry is better expressed by a term of the form L/d(L+d), as already proposed in ref. (3), where L represents the length of the straight section considered and d the distance from its end. This is clearly shown in Figs. 3 and 4 for the

fluence and absorbed dose rate respectively, normalized to 1 e^-/s, for a 10 m long straight section operating at a pressure of $1.33 \cdot 10^{-7}$ Pa (10^{-9} torr).

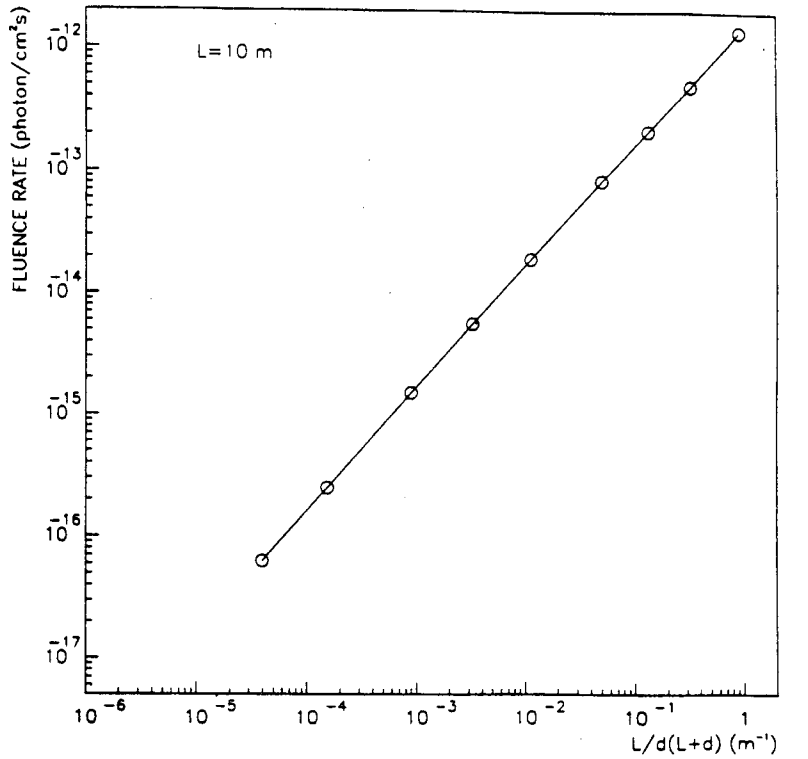

FIG. 3 – Fluence rate per e^-/s as a function of L/d(L+d) in the case of a straight section 10 m long operating at $1.33 \cdot 10^{-7}$ Pa (10^{-9} torr). Primary electron energy 510 MeV.

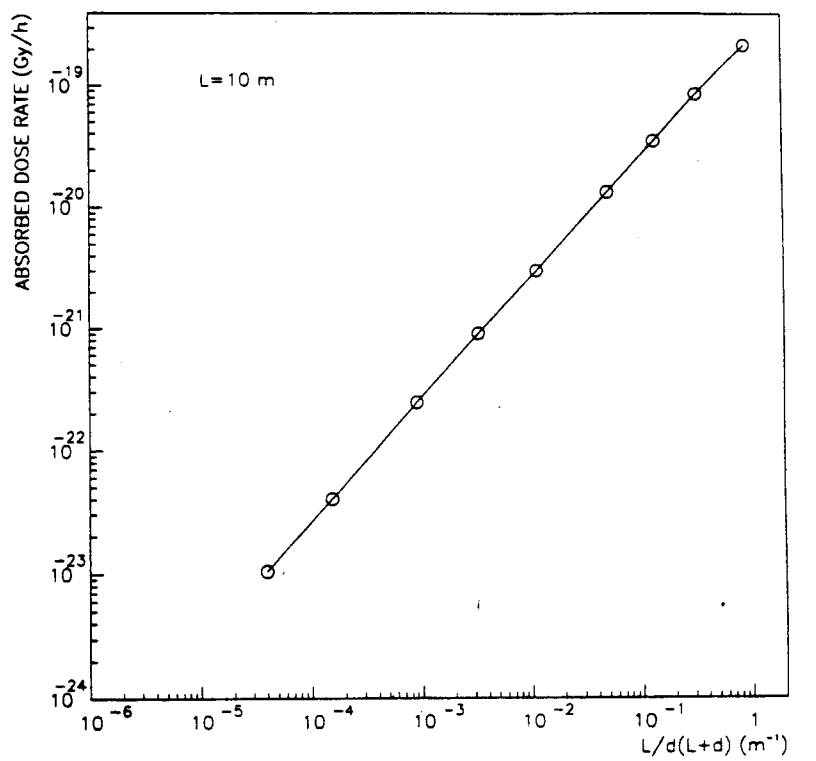

FIG. 4 – Absorbed dose rate per e^-/s as a function of L/d(L+d) in the case of a straight section 10 m long operating at $1.33 \cdot 10^{-7}$ Pa (10^{-9} torr). Primary electron energy 510 MeV.

The linear dependence of fluence rate and absorbed dose rate on the term L/d(L+d) has been verified in the whole range of lengths considered. The accuracy in the choice of the exponent 1 for the term L/d(L+d) is better than 1%.

However, the slope of the straight lines, based on data linearly extrapolated to $1.33 \cdot 10^{-7}$ Pa (10^{-9} torr) from the results of FLUKA simulation at atmospheric pressure, is practically constant for L≤10 m while for longer straight sections it slightly decreases as L increases. This was easily explained by the failure of the above mentioned conditions on electron and photon mean free paths for such long straight sections: further simulations performed with a reduced pressure (1/10 atm) allowed to verify that the slope remains constant also for straight sections longer than 10 m.

As concerns the dependence on the electron energy, Fig. 5 and Fig. 6 show the fluence rate and the absorbed dose rate respectively, normalized to 1 e^-/s, as a function of L/d(L+d), for different primary electron energies, in the case of a straight section 1 m long at a pressure of $1.33 \cdot 10^{-7}$ Pa (10^{-9} torr). The linear dependence of fluence rate and absorbed dose rate on L/d(L+d) is always verified.

For a given value of the term L/d(L+d), the fluence rate rises with the energy according to E^2 and the absorbed dose according to $E^{2.67}$. The different functional dependence of the two quantities on E reflects the energy dependence of the conversion coefficients.

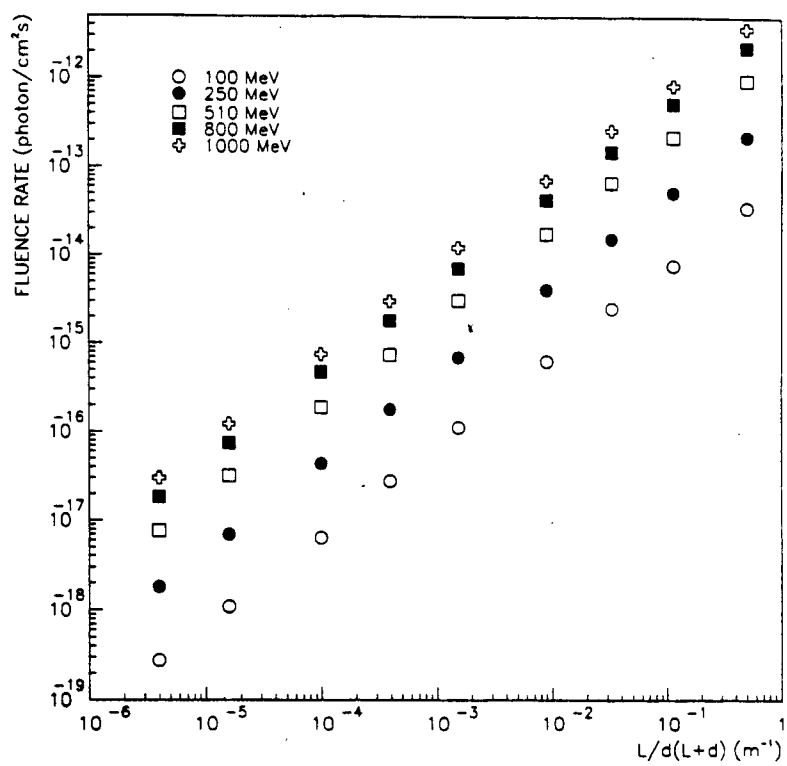

FIG. 5 – Fluence rate per e^-/s as a function of L/d(L+d) in the case of a straight section 1 m long operating at $1.33 \cdot 10^{-7}$ Pa (10^{-9} torr) for different energies of the primary electron beam.

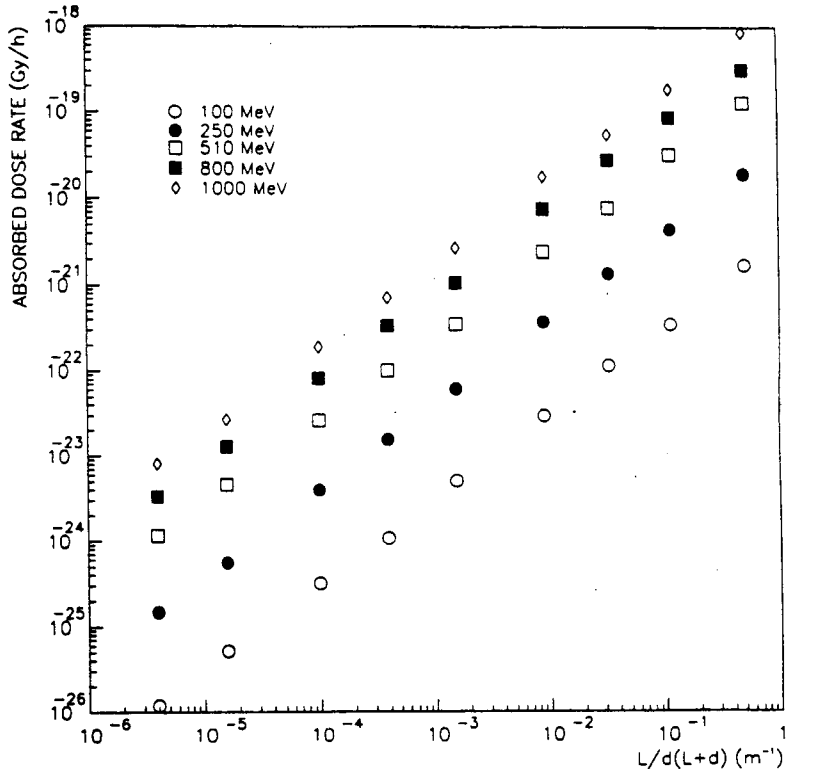

FIG. 6 – Absorbed dose rate per e^-/s as a function of L/d(L+d) in the case of a straight section 1 m long operating at $1.33 \cdot 10^{-7}$ Pa (10^{-9} torr) for different energies of the primary electron beam.

The results described above allow to propose the following expression relating the fluence rate φ, expressed in $cm^{-2}\ s^{-1}$, the primary electron energy E (MeV), the beam current I (e^-/s), the pressure p (Pa), the straight section length L (m) and the distance (d):

$$\varphi = 1.9 \times 10^{-18} \left(\frac{E}{mc^2}\right)^2 \frac{L}{d(L+d)}\, I \frac{p}{p0} \qquad (1)$$

where mc^2=0.511 MeV and $p_0 = 1.33 \cdot 10^{-7}$ Pa (10^{-9} torr).

We remind that the particle fluence is the fundamental quantity in radiation dosimetry. The knowledge of the fluence rate through eq. (1), joined to the spectra shown in Fig. 2, allows to get every information required for radiation protection purposes, included the absorbed dose itself, whatever the conversion coefficients may be.

Likewise, using the conversion coefficients suggested by Rogers (19), the following expression is proposed for the absorbed dose rate $\dot{D}$ (Gy/h):

$$\dot{D} = 2.5 \times 10^{-27} \left(\frac{E}{mc^2}\right)^{2.67} \frac{L}{d(L+d)}\, I \frac{p}{p0} \qquad (2)$$

where the symbols have the same meaning as in eq. 1.

At last, we have studied the validity of eq. (1) and (2) at distances lower than 1 m.

At 1 mm from the end of the straight section the behaviour of fluences and doses as a function of the radius of the detector, at least for the radii here investigated, is no more similar to the one shown in Fig. 1. The two quantities become independent on the length of the straight section and increase steadily as the radius of the detector decreases. This can be easily explained by the fact that the angle covered by the detector with respect to interactions in the last part of the target is always larger than the characteristic one. As a consequence, even a 5 μm detector becomes too large.

At a distance of 10 cm the curves are already similar to those shown in Fig. 1, but fluence and absorbed dose evaluated from eq. (1) and (2) are lower than those found in the simulation of 5% – 40% depending on the straight section length.

Finally from a distance of 20 cm eq. (1) and (2) and results of simulation are in good agreement.

In conclusion the suggested equations can be applied from 20 cm over. At lower distances, however, even the pencil beam approximation is no longer valid due to beam emittance effects.

A comparison between measured and calculated results requires the knowledge of the actual pressure in the vacuum chamber which is very difficult to measure. The discrepancies between the pressure measured by vacuum gauges in a storage ring and the effective pressure can be due to various reasons such as electric discharge in ion pumps, ion trapping in the stored beam, pressure rise due to synchrotron radiation, etc (12,21,2).

Nevertheless we have tried to compare the results of our calculations with measurements performed at ADONE some years ago (3). In the case of a stored beam of 550 MeV, the absorbed dose rate measured at 9 m of distance from a 6 metre long straight section operating at a pressure of $1.33 \cdot 10^{-7}$ Pa (10^{-9} torr), behind a 12 mm steel thickness, was $2.3 \cdot 10^{-5}$ Gy/h·mA (3). Using eq. (1) it would be $8.6 \cdot 10^{-5}$ Gy/h · mA. The agreement between the two results is reasonably good, if one takes into account the attenuation introduced by the steel, the effect of beam size and above all the possible discrepancies between effective pressure in the path of electrons and pressure measured by vacuum gauges during the measurement.

CONCLUSIONS

The proposed equations can be very useful for estimating the absorbed dose produced by gas bremsstrahlung. In particular, eq. (1) joined to the spectra shown in Fig. 2 allows to get any useful information for health physics purposes, including the absorbed dose rate itself, if the conversion coefficients adopted here were judged inadequate or too conservative. As concerns the comparison with experiments, the typical uncertainties on the pressure in the electron path make difficult any absolute comparison. However, relative measurements could be useful in establishing the validity of the proposed dependences on the distance and on the straight section length.

REFERENCES

(1) A. Rindi, Health Physics, **42** (1982) 891.

(2) H. Kobayakawa, K. Huke, M. Izawa, Y. Kamiya, M. Kihara, M. Kobayashi and S. Sakanaka, Nucl. Instr. Meth., **A248** (1986) 565.

(3) A. Esposito and M. Pelliccioni, LNF-86.23(NT) (1986).

(4) A. Esposito and M. Pelliccioni, in: Health Physics of Radiation Generating Machines. Proceedings of the Health Physics Society, Reno, CONF-8602106, (1987) 495.

(5) P. M. De Luca, R. A. Otte, W. P. Swanson, S. W. Schilthelm and G. Rogers, in: Health Physics of Radiation Generating Machines. Proceedings of the Health Physics Society, Reno, CONF-8602106, (1987) 486.

(6) M. Holbourn, Internal Note, Daresbury, HS85/151 (1985).

(7) S. Sakanaka, M. Izawa, H. Kobayakawa and M. Kobayashi, Nucl. Instr. Meth., **A256** (1987) 184.

(8) R. Ryder and M. P. Holbourn, Addendum to HP81/139 (1981).

(9) K. Batchelor ed., National Synchrotron Light Source Safety Analysis Report, Brookhaven National Laboratory, (1982).

(10) M. Holbourn, Internal Note, Daresbury, HP81/139 (1981).

(11) W. P. Swanson, P. M. De Luca, R. A. Otte and S. W. Schilthelm, Aladdin Upgrade Design Study: Shielding, April 23 (1985).

(12) S. Ban, H. Hirayama and S. Miura, Health Physics, **57** (1989) 407.

(13) G. Tromba and A. Rindi, Nucl. Instr. Meth. in Phys. Res., **A292** (1990) 700.

(14) A. Fassò, A. Ferrari, J. Ranft, P.R. Sala, G.R. Stevenson and J. M. Zazula, FLUKA92, presented at the Workshop on Simulating Accelerator Radiation Environments, 11-15 January 1993, Santa Fe.

(15) A. Ferrari, P.R. Sala, A. Fassò and G.R. Stevenson, Proc. II Int. Conf. on Calorimetry in High Energy Physics (1991).

(16) A. Ferrari, P.R. Sala, G. Guaraldi and F. Padoani, Nucl. Instr. Meth., **B71** (1992) 412.

(17) A. Ferrari and P.R. Sala, Improvements to the Electromagnetic Part of the FLUKA Code, to be published.

(18) S.M. Seltzer and M.J. Berger, Atomic Data and Nuclear Data Tables, **35** (1986) 345.

(19) D. W. O. Rogers, Health Physics, Vol. **46**, No. 4 (1984) 891.

(20) A. Ferrari, M. Pelliccioni and P.R. Sala, Nucl. Instr. Meth., B (in press).

(21) M. Kobayashi, K. Huke, S. Ban and H. Hirayama, in: Proceedings of the 5th Symposium on Accelerator Science and Technology. Tsukuba, Japan (1984) 148.

(22) H. W. Koch and J. W.~Motz, Rev. Mod. Phys., **31** 4 (1959) 920.

(23) A.F. Bielajev, R. Mohan and C.S. Chui, National Research Council of Canada, Internal Report PIRS-0203 (1989).